

Accumulation of Terrestrial Dissolved Organic Matter Potentially Enhances Dissolved Methane Levels in Eutrophic Lake Taihu, China

Yongqiang Zhou,^{†,‡,§,○} Qitao Xiao,^{†,○} Xiaolong Yao,^{†,‡} Yunlin Zhang,^{*,†,‡} Mi Zhang,^{||} Kun Shi,^{†,‡} Xuhui Lee,^{||} David C. Podgorski,^{⊥,○} Boqiang Qin,^{†,‡} Robert G. M. Spencer,[#] and Erik Jeppesen^{§,▽}

[†]State Key Laboratory of Lake Science and Environment, Nanjing Institute of Geography and Limnology, Chinese Academy of Sciences, Nanjing 210008, China

[‡]University of Chinese Academy of Sciences, Beijing 100049, China

[§]Sino–Danish Centre for Education and Research, Beijing 100190, China

^{||}Yale–NUIST Center on Atmospheric Environment, International Joint Laboratory on Climate and Environment Change (ILCEC), Nanjing University of Information Science and Technology, Nanjing 210044, China

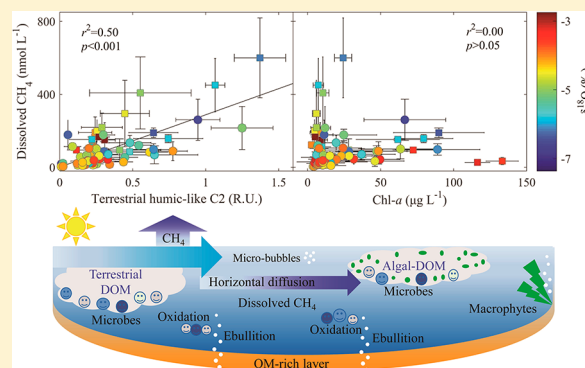
[⊥]Pontchartrain Institute for Environmental Sciences, Department of Chemistry, University of New Orleans, New Orleans 70148, Louisiana United States

[#]Department of Earth, Ocean and Atmospheric Science, Florida State University, Tallahassee, Florida 32306, United States

[▽]Department of Bioscience and Arctic Research Centre, Aarhus University, Vejlsovej 25, DK-8600 Silkeborg, Denmark

Supporting Information

ABSTRACT: Inland waters play an important role for the storage of chromophoric dissolved organic matter (CDOM) and outgassing of methane (CH₄). However, to date, linkages between the optical dynamics of CDOM and dissolved CH₄ levels remain largely unknown. We used multi-year (2012–2014) seasonal data series collected from Lake Taihu and 51 connecting channels to investigate how CDOM optical dynamics may impact dissolved CH₄ levels in the lake. High dissolved CH₄ in the northwestern inflowing river mouths coincided with high underwater UV–vis light availability, dissolved organic carbon (DOC), chemical oxygen demand (COD), DOM aromaticity, terrestrial humic-rich fluorescence, in situ measured terrestrial CDOM, depleted dissolved oxygen (DO), stable isotopic δ²H, and δ¹⁸O compared with other lake regions. Our results further revealed positive relationships between dissolved CH₄ and CDOM absorption at 350 nm, i.e. *a*(350), COD, DOC, terrestrial humic-rich fluorophores, and DOM aromaticity, and negative relationships between dissolved CH₄ and DO, δ²H, and δ¹⁸O. The central lake samples showed a major contribution of terrestrial-sourced molecular formulas to the ultrahigh resolution mass spectrometry data, suggesting the presence of allochthonous DOM sources even here. We conclude that an elevated terrestrial CDOM input likely enhances dissolved CH₄ levels in Lake Taihu.



INTRODUCTION

Inland waters (rivers, lakes, ponds, etc.) play an important role for the storage and outgassing of greenhouse gases.^{1,2} Lake ecosystems, especially the most common shallow lake types, are hot spots of organic carbon transformation and methane (CH₄) emission.³ Globally, lakes cover 3.7% of the Earth's ice-free land surface area and contribute approximately 20% of the CH₄ outgassing from all natural ecosystems.⁴ Eutrophication and climate warming have together fueled the outgassing of CH₄ from lake ecosystems.^{3,5} The net outgassing of CH₄ from lakes to the atmosphere is the difference between methanogenesis and oxidation of CH₄.^{6,7} Anaerobic fermentation of acetate by certain archaea (acetoclastic methanogenesis) in carbon-rich environments serving as the terminal step in the

decomposition of dissolved organic matter (DOM) has traditionally been considered as the primary pathway of biological CH₄ production.^{6,7} However, recent studies have highlighted that a large fraction of CH₄ oversaturation in aquatic environments can be produced in oxygenated surface waters.^{8,9} The paradoxical supersaturation of CH₄ in oxygenated surface waters has been suggested to be a result of microbial transformation of DOM.^{8,9} Recent studies have also suggested that photochemical degradation may be more

Received: April 23, 2018

Revised: August 14, 2018

Accepted: August 24, 2018

Published: August 24, 2018

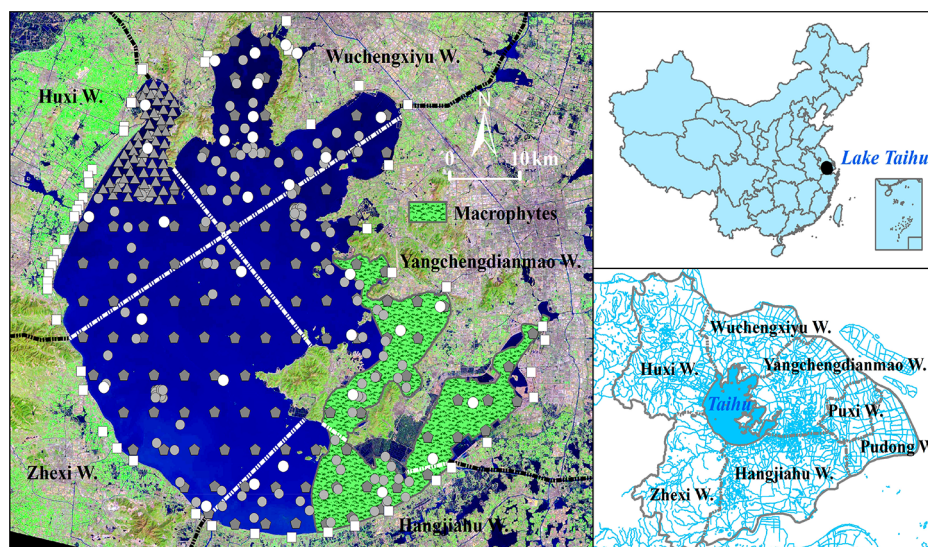


Figure 1. Location of 32 seasonal sampling sites from February 2012 to November 2014 (white circles) in Lake Taihu (the sites were divided into five spatial subgroups delineated by white dashed lines following the boundaries of the five corresponding subwatersheds); seasonal sampling sites on the 51 major rivers/channels connecting to the lake from February 2013 to November 2014 (white quadrates); 51 sites sampled in northwestern Zhushan Bay in May 2014 (gray triangles); 146 sites sampled in October 2008 (gray circles); 116 sites sampled in January and June 2014 and in June 2015 (gray pentagons). Shadowed areas denote the macrophyte-dominated regions in Lake Taihu according to Dong et al.⁴⁷ and Liu et al.⁴⁸

important than microbial degradation in controlling the decomposition of newly exposed terrestrial DOM, further stimulating the outgassing of greenhouse gases in Arctic waters.^{10,11} Irradiation experiments revealed significant photochemical CH_4 production in the anoxic water column,¹² especially in the inflowing river mouths in this case.

DOM plays a vital role in biogeochemical processes in inland waters and the composition of lake DOM is highly variable, depending on its source, biological reactivity, and time of processing.^{13,14} Terrestrial humic-rich substances usually contribute primarily to the DOM pool in lakes in the monsoon region, while autochthonous inputs from algae and macrophytes can also be important substrates for microbial loop.^{13–15} Both terrestrial and autochthonous DOM can be utilized and transformed by microbial and photochemical degradation and are important sources of carbon in lake ecosystems.^{16,17} The mixing of terrestrial and autochthonous algal-derived chromophoric dissolved organic matter (CDOM) in inflowing river mouths can further result in enhanced degradation of carbon and nitrogen in lakes, known as the priming effect.¹⁸ Terrestrial humic-rich substances including polycyclic aromatics and vascular-plant-derived polyphenols are photoreactive and photochemical degradation augments the lability of CDOM to the subsequent biological degradation,¹⁴ with CH_4 being released as byproduct.^{8,9} Urbanization, industrialization, and conversion of land to agriculture have led to increased discharge of domestic sewage and agricultural and industrial effluents to lakes, which likely enhances microbial- and photochemical-induced oxygen depletion of the river mouth water column.¹⁶ The susceptibility of DOM to microbial and photochemical degradation in aquatic ecosystems depends largely on its sources and chemical composition.¹⁹ Oxygen depletion in river mouths resulting from an augmented terrestrial DOM input has, however, lowered bacterial and archaea oxidation of CH_4 (aerobic and anaerobic, respectively) to CO_2 , a major pathway of biological CH_4 oxidation, consequently reducing the levels of dissolved

CH_4 .²⁰ To date, however, the role of the composition of DOM for the levels of dissolved CH_4 in lake ecosystems remains to be elucidated.

Lake Taihu is well-suited for the undertaking of studies to reveal the linkage between CDOM optical dynamics and dissolved CH_4 levels as it has high inputs of both allochthonous and autochthonous DOM. The Lake Taihu watershed is located in the Yangtze River Delta, the most urbanized area in China with a high population density and extensive economic development. Excessive input of nutrients has led to the occurrence and persistence of nuisance blooms of cyanobacteria and high heterogeneity of DOM quality and dissolved CH_4 concentrations in the lake.²¹ The direction of the water flow of the channels connecting Lake Taihu with the fluvial plain is primarily controlled by meteorological and anthropogenic disturbances (e.g., floodgates).²² However, to date, the relative importance of allochthonous and autochthonous CDOM, regulated by the inflow and backflow discharge (Q_{net} , net inflow discharge), for the dissolved CH_4 levels has not been assessed.

We studied how the optical compositional dynamics of CDOM mediated by net inflow discharge quantitatively drives the levels of dissolved CH_4 . A total of 700 CDOM samples and 552 headspace CH_4 samples were collected in Lake Taihu and the connecting channels in the watershed from February 2012 to November 2014. We expected to find large variations in dissolved CH_4 levels among lake regions and hydrological seasons due to different net inflow of terrestrial CDOM.

■ MATERIALS AND METHODS

Study Sites. Lake Taihu has an area of 2338.1 km^2 and a water retention time of ~ 309 days,²³ and the lake watershed covers 36 500 km^2 . A total of 172 channels are connected with the lake, and the elevation of the water surface of the connecting channels is mostly lower than 5 m.²⁴ The water exchange between the lake and the connecting channels is complex and similar to that of lagoons. This leads to large

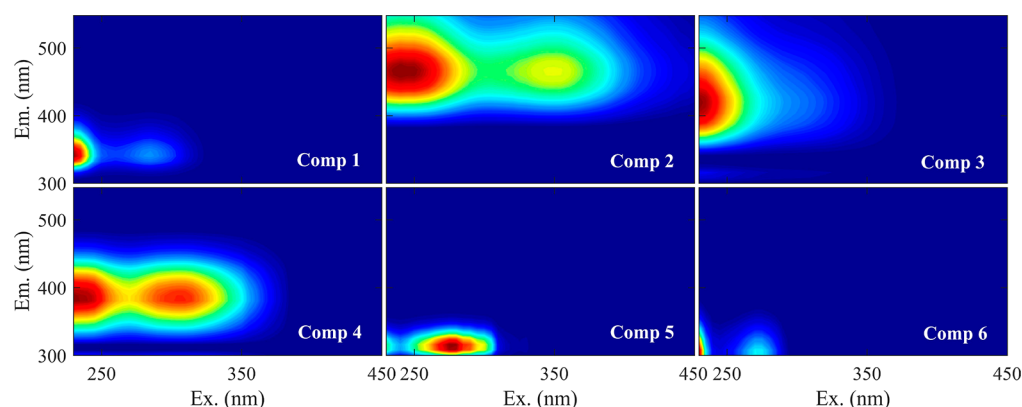


Figure 2. Spectral shapes of the six PARAFAC-derived components (C1–C6). The model was well validated by the split-half validation procedure (Figure S4).

variations in the concentration and composition of DOM in different areas of the lake. Information about hydraulic subwatersheds and hydrological data collection, multiyear variations of daily $\delta^2\text{H}$ and $\delta^{18}\text{O}$ (Figure S2), and monthly Q_{net} (inflow – backflow runoff) in each hydraulic subwatershed (Figure S3; Table S1) can be found in the [Supporting Information](#).

Light Availability, Secchi Disk Depth (SDD), Dissolved Oxygen (DO), and CDOM Optical Sampling Collection. Water depth (WD) was measured in situ using a scaled straight stick, while Secchi disk depth (SDD) was determined in situ using a 30 cm diameter black and white Secchi disk. The dissolved oxygen (DO) concentration was determined in situ at 0.5 m depth using a YSI 6600 V2 multisensor sonde. WD, SDD, and DO data were only available from the seasonal campaign conducted in Lake Taihu from February 2012 to November 2014 (Table S2).

CDOM absorption and fluorescence measurements were conducted to trace the sources and optical properties of CDOM and to investigate the impacts of CDOM optical compositional dynamics on the levels of dissolved CH_4 . Detailed information about the seasonal CDOM sampling collection in the lake and the connecting channels from 2012 to 2014 can be found in the [Supporting Information](#) (Table S2).

Previous studies have revealed that relatively high concentrations of dissolved organic carbon (DOC) are exported to Lake Taihu from the northwestern subwatershed via Zhushan Bay.^{25,26} An extensive sampling campaign ($n = 61$) was therefore carried out in Zhushan Bay, located in northwestern Lake Taihu, in April 2014 with the aim to trace the sources of CDOM and assess light availability (Figure 1). Detailed information about the measurement of CDOM fluorescence using an in situ CDOM fluorescence sensor, light availability indices including the diffuse attenuation coefficient, K_d , of light in the UV region and the photosynthetically active radiation (PAR, 400–700 nm), as well as measurements of total suspended matter (TSM) and inorganic suspended matter (ISM), can be found in the [Supporting Information](#) (Table S2).

Stable Isotopic $\delta^2\text{H}$ and $\delta^{18}\text{O}$ Sampling Collection and Measurements. Stable isotopic composition of surface water provides information on hydrological and meteorological processes as evaporation fuels the accumulation of the heavier isotopic water molecules (H^2HO and H_2^{18}O) in the liquid water,²⁷ and these can therefore be used to trace the sources of

riverine CDOM and evaporation in Lake Taihu. We assumed that the source of riverine CDOM in Lake Taihu is consistent with the depletion of $\delta^2\text{H}$ and $\delta^{18}\text{O}$. Detailed information about the stable isotopic $\delta^2\text{H}$ and $\delta^{18}\text{O}$ sampling collection in the lake and the connecting channels can be found in the [Supporting Information](#) (Table S2).

Chlorophyll *a* (Chl-*a*), Chemical Oxygen Demand (COD), DOC, and CDOM Optical Measurements. Previous studies have indicated that the degradation of algal mats can impact the levels of dissolved CH_4 .^{1,3,21} In this study, Chl-*a* was used as a surrogate for algal biomass, and the linkage between Chl-*a* and dissolved CH_4 concentrations in Lake Taihu was investigated. DOC, COD, and optical measurements of CDOM were used to trace the sources and optical composition of CDOM (for information about Chl-*a*, DOC, COD, and CDOM optical measurements, see the [Supporting Information](#), Table S2).

CDOM absorption indices included the absorption coefficient at 350 nm, $a(350)$, the ratio of $a(250)/a(365)$, the spectral slope ($S_{275-295}$), and the slope ratio (S_R), which can be used to trace the amount of CDOM^{17,19,28} and the relative molecular size and aromaticity of CDOM.^{29,30} Detailed information about the measurement and calculation of CDOM absorption indices is given in the [Supporting Information](#) (Table S2).

CDOM fluorescence (excitation–emission matrixes, EEMs) measurements and the calibration processes including corrections of Raman and Rayleigh peaks, inner-filter effects, and normalization of Raman units (RU) can be found in the [Supporting Information](#). PARAFAC is a three-way multivariable data analysis technique that statistically decomposes the complex mixture of CDOM fluorophores into trilinear components with a single emission maximum and corresponding to a group of highly covarying analytes.^{31,32} Using PARAFAC modeling, a six-component model was well validated (Figure 2; Figures S4 and S5) (see details about the modeling and validation in the [Supporting Information](#), Table S2).

Dissolved CH_4 Sampling Collection and Measurements. In total, dissolved CH_4 concentrations were determined in 552 headspace samples (29 lake sites \times 4 seasons \times 3 years and 51 river sites \times 4 seasons) (Figure 1; Table S2). Direct measurement of dissolved CH_4 was performed by headspace equilibration following the method detailed in Xiao et al.²¹ (see the [Supporting Information](#), Table S2). We determined only the levels of dissolved CH_4 but not

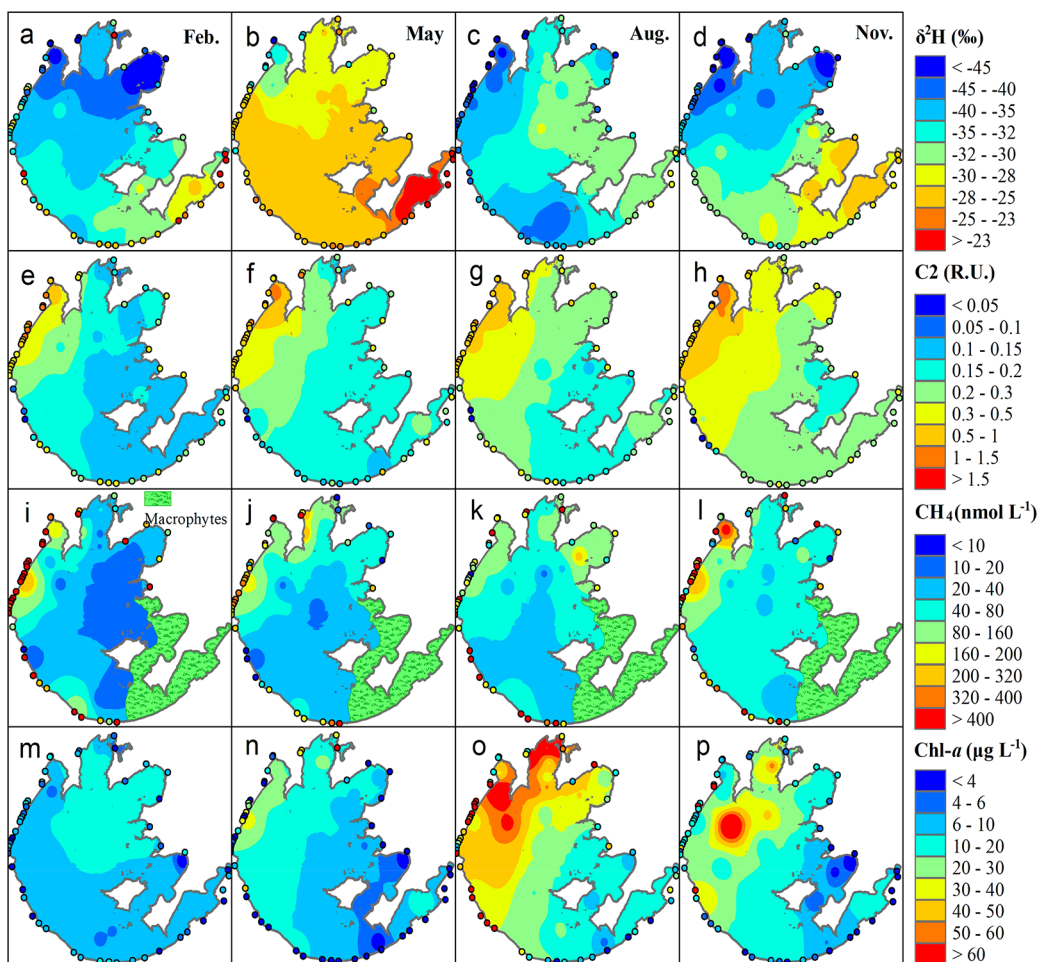


Figure 3. Spatial variations of multiyear (2012–2014) mean stable isotopic $\delta^2\text{H}$ (a–d); F_{max} of terrestrial humic-like C2 (e–h), dissolved methane (CH_4 , i–l), and chlorophyll *a* (Chl-*a*) concentrations (m–p) in Lake Taihu; and 51 major connecting channels in February, May, August, and November. Data on CH_4 and Chl-*a* in the samples collected in connecting channels were only available for May, August, and November 2013 and February 2014.

CH_4 emission as wind speed and flow velocity data for the river samples were not available. Although the relationship between the levels of dissolved CH_4 and CH_4 emissions is not 1:1, in this study we used dissolved CH_4 concentrations as a proxy for the potential CH_4 emission flux in different areas of Lake Taihu since the levels of dissolved CH_4 largely control the emission from the lake²¹ (Figure S1).

Fourier Transform Ion Cyclotron Resonance Mass Spectrometry (FT-ICR MS) Analyses. Details on the pretreatment of the FT-ICR MS samples can be found in the Supporting Information. Briefly, in November 2016, FT-ICR MS samples collected from central Lake Taihu and headwater streams of the lake basin as well as algal-derived samples to determine degradation were solid-phase-extracted with PPL Bond Elut (Agilent) resins before analysis by negative-ion electrospray FT-ICR MS^{33,34} to trace the sources of DOM in the lake. Different sources of CDOM exhibit distinct molecular signatures,³⁵ and FT-ICR MS can be a useful tool in tracing the sources of CDOM in Lake Taihu.

The assigned molecular formulas were categorized according to Ohno et al.³⁶ Briefly, the chemical classes classified by the van Krevelen diagrams include the following: (i) lipids (O/C = 0–0.3, H/C = 1.5–2.0), (ii) proteins and amino sugars (O/C = 0.3–0.67, H/C = 1.5–2.2), (iii) lignins (O/C = 0.1–0.67, H/C = 0.7–1.5), (iv) carbohydrates (O/C = 0.67–1.2, H/C =

1.5–2.2), (v) unsaturated hydrocarbons (O/C = 0–0.1, H/C = 0.7–1.5), (vi) condensed aromatics (O/C = 0–0.67, H/C = 0.2–0.7), and (vii) tannins (O/C = 0.67–1.2, H/C = 0.5–1.5).³⁶

Statistical Analyses. Statistical analyses, including mean values, standard deviations (SD), and *t*-tests, were performed applying R-studio 0.97.551 (R i386 2.15.2) software. Linear regressions and van Krevelen diagrams were made using MATLAB R2016b. Results with $p < 0.05$ for *t*-tests and linear regressions were reported as significant. Means were shown \pm SD.

RESULTS

PARAFAC Modeling Results. Fluorescent DOM (FDOM) is composed of humic substances and amino acids, both free and bound in proteins, and alterations in PARAFAC-derived FDOM components are sometimes used as a surrogate for changes in the composition of the wider DOM pool.³² The six-component PARAFAC model explains >99.9% of the variables of the whole EEMs data set. The spectral characteristics of the six components (C1–C6, Figure 2; Figure S4) were compared with PARAFAC results for samples collected from other aquatic ecosystems using an online spectral library called Openfluor.³⁷ C1 had two Ex maxima at ≤ 230 and 285 nm and an Em maximum (340 nm) as have amino acid

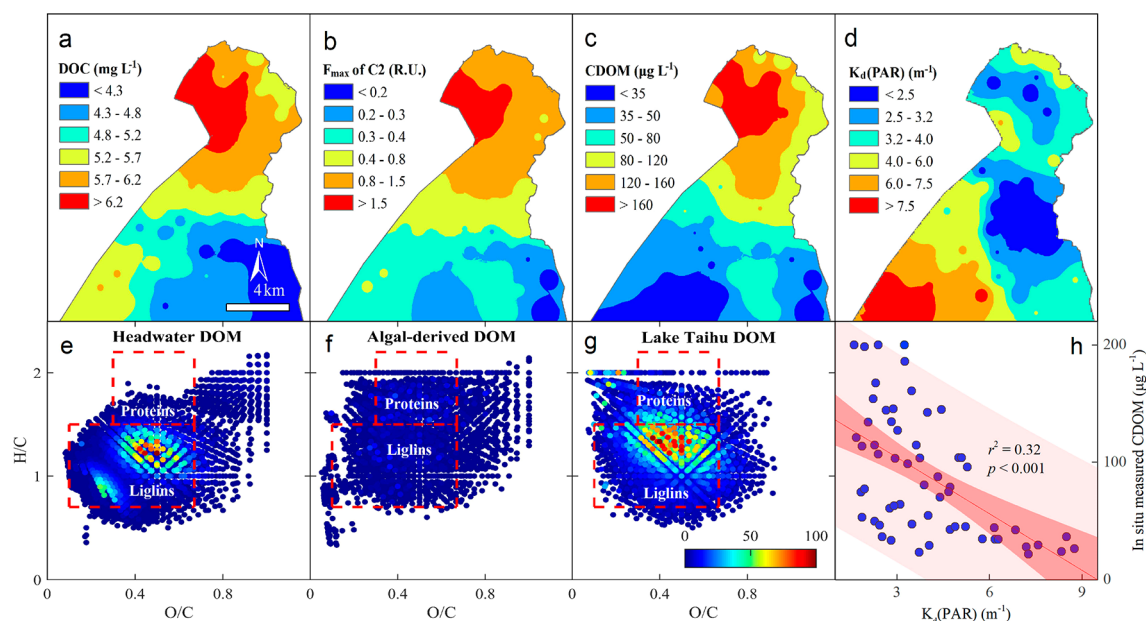


Figure 4. Spatial variations of dissolved organic carbon (a), F_{\max} of terrestrial humic-like C2 (b), terrestrial CDOM concentrations measured using an in situ fluorescence sensor (c), and diffuse attenuation coefficient of PAR ($K_d(\text{PAR})$) (d) in Zhushan Bay, northwestern Lake Taihu, in April 2014. Examples of van Krevelen diagrams based on the distribution of headwater DOM (e), algal-derived DOM (f), and central Lake Taihu DOM (g) samples. Dashed boxes in panels e–g tentatively assigned as protein and lignin molecules are marked. Relationship between $K_d(\text{PAR})$ and terrestrial CDOM concentrations measured using fluorescence sensor (h). The colored dots in the lower three panels represent the percent relative abundance of the FT-ICR MS signals. Relationship between $K_d(\text{PAR})$ and in situ measured CDOM concentrations (h).

associated tryptophan-like components.^{38,39} C2 displayed two Ex maxima at 240 and 350 nm and an Em maximum (468 nm) and is categorized as a typical terrestrial humic-like substance.^{13,38,40–42} C3 exhibited Ex/Em maxima at $\leq 230/420$ nm, similar to those of agricultural-soil-derived humic-like or fulvic-like materials.^{40,42–44} C4 peaked at 380 nm and is categorized as a microbial humic-like substance.^{38,44,45} C5 (Ex/Em ≤ 230 (275)/316 nm) and C6 (Ex/Em ≤ 230 (270)/ ≤ 300 nm) had spectral characteristics similar to those of red-shifted tyrosine and typical tyrosine substances, respectively.^{38,46} The multiyear (2012–2014) mean F_{\max} ranged from 0.24 ± 0.09 RU (microbial humic-like C4) to 5.04 ± 2.04 RU (tryptophan-like C1) for the PARAFAC-derived C1–C6 in Lake Taihu with the relative contribution percentages for the six components ranging from $2.2 \pm 0.8\%$ (C4) to $46.9 \pm 19.0\%$ (C1) (Table S3).

Spatial Variability of Light Availability, Stable Isotopic $\delta^2\text{H}$ and $\delta^{18}\text{O}$, CDOM-Related Indices, COD, DO, Dissolved CH_4 , and Chl-*a*. SDD in the lake ranged from 0.0 to 1.7 m with a mean of 0.4 ± 0.3 m, high values being observed in the northern and northwestern bays for the campaigns conducted seasonally from February 2012 to November 2014 (Figure S6). The ratio of SDD to WD ranged from 0.06 to 0.61 with a mean of 0.19 ± 0.12 and, similarly, high values of the ratio of SDD to WD were recorded in the northern and northwestern bays of the lake (Figure S6).

As evaporation enhances the accumulation of heavier water isotopic molecules of $\delta^2\text{H}$ and $\delta^{18}\text{O}$ in the liquid water, more depleted $\delta^2\text{H}$ and $\delta^{18}\text{O}$ imply a strong riverine signal, while enriched $\delta^2\text{H}$ and $\delta^{18}\text{O}$ indicate evaporation induced by prolonged water retention time in the lake.²⁷ For all samples collected from 2012 to 2014, $\delta^2\text{H}$ and $\delta^{18}\text{O}$ ranged from -63.4 to -16.5% ($-33.9 \pm 8.2\%$) and from -8.9 to 0.4% ($-4.6 \pm 1.3\%$), respectively. Multiyear mean $\delta^2\text{H}$ and $\delta^{18}\text{O}$ increased notably from the northwestern bays to the southeastern bays in

all seasons (Figure 3; Figure S7). $\delta^2\text{H}$ and $\delta^{18}\text{O}$ in the samples collected from the inflowing rivers, i.e., in the northwestern subwatersheds (e.g., Huxi and Wuchengxiyu) were generally lower than in the corresponding bays and coastal lake regions.

In all samples collected from 2012 to 2014, DOC and $a(350)$ ranged from 1.0 to 17.2 mg L^{-1} ($4.4 \pm 1.3 \text{ mg L}^{-1}$) and from 0.4 to 16.0 m^{-1} ($4.0 \pm 1.6 \text{ m}^{-1}$), respectively. Multi-year (February 2012 to November 2014) mean concentrations of DOC and $a(350)$ and the F_{\max} of C1–C4 and C6 decreased markedly from the northwestern part of the lake, especially Zhushan Bay, to the southeastern lake regions (Figure 3; Figure S7). In comparison, $a(250)/a(365)$, $S_{275-295}$, and S_R increased notably from the northwestern part of the lake to the southeastern bays (Figure S7). COD concentrations in the samples collected from the lake from 2012 to 2014 ranged from 2.43 to 15.56 mg L^{-1} with a mean of $4.27 \pm 1.28 \text{ mg L}^{-1}$, and COD decreased gradually from the northwestern regions to the southeastern bays in all seasons (Figure S6). DO concentrations in the samples collected from the lake ranged from 2.47 to 12.28 mg L^{-1} with a mean of $8.86 \pm 1.69 \text{ mg L}^{-1}$, and depleted DO was observed in the northwestern inflowing river mouths (Figure S6).

Zhushan Bay located in northwestern Lake Taihu has relatively high concentrations of terrestrial, agricultural, and microbial humic-like fluorophores as well as depleted DO (Figure 3; Figure S6), and the sources of CDOM in the bay were investigated based on more comprehensive samplings.²⁵ The exclusively terrestrial humic-like C2 decreased from the northwestern Zhushan Bay and the northeastern coastal lines to the southeastern bays in all seasons from 2012 to 2014 (Figures 3 and 4), coinciding with the higher inflow runoff from the tributaries in the Huxi and Wuchengxiyu subwatersheds than in the remaining subwatersheds. During the Zhushan Bay sampling campaign in April 2014, DOC ranged from 3.7 to 7.1 mg L^{-1} with a mean of $5.3 \pm 0.8 \text{ mg L}^{-1}$

(Figure 4). In comparison, F_{\max} of terrestrial humic-like C2 and in situ measured fluorescence intensity (370/460 nm) ranged from 0.1 to 2.7 RU (0.8 ± 0.6 RU) and from 21.5 to 200.0 $\mu\text{g L}^{-1}$ (90.8 ± 54.2 $\mu\text{g L}^{-1}$), respectively (Figure 4). DOC concentrations, F_{\max} of terrestrial humic-like C2, and measured in situ fluorescence intensity (370/460 nm) all decreased notably from the northwestern inner Zhushan Bay toward the south entrance of the bay (Figure 4). The sampling in Zhushan Bay therefore indicated that high concentrations of terrestrial humic-like and anthropogenic tryptophan-like fluorophores were discharged into the lake via the bay, potentially enhancing the levels of dissolved CH_4 . K_d of light in the UV region and the PAR regions was fairly low, corresponding to a relatively low TSM and high SDD at the inflowing river mouth compared with the open water region (Figure 4; Figures S6 and S8). Correspondingly, a significant negative relationship was found between the K_d of light in the UV region and the PAR regions and SDD ($r^2 = 0.89$, $p < 0.001$) and with in situ measured fluorescence intensity (370/460 nm) ($r^2 = 0.32$, $p < 0.001$) (Figure 4; Figure S8).

Dissolved CH_4 samples collected from the macrophyte-dominated lake regions (Figure 1) were excluded from our analyses since macrophytes influence the dynamics of the greenhouse gas exchange.^{1,3} Submerged macrophytes affect biological and chemical processes in shallow lakes, including the biomass of organisms across trophic levels, and can therefore affect the dynamics of greenhouse gas.¹ Submerged macrophytes fuel the transport of dissolved and ebullitive CH_4 from the sediment to the water column and can thus increase dissolved CH_4 concentrations in the water.³ This is supported by a recent study showing that organic sediments in macrophyte-dominated lake areas strongly enhanced the levels of dissolved CH_4 .²¹ In this study, the boundaries of macrophyte-dominated lake regions were delineated following the results detailed in Dong et al.⁴⁷ and Liu et al.⁴⁸ (Figure 1). The field investigation conducted by Dong et al.⁴⁷ showed that East Lake Taihu Bay, Xukou Bay, and Guangfu Bay in the southeastern part of the lake were macrophyte-dominated, which was well validated by the remote sensing results obtained by Liu et al.⁴⁸ Dissolved CH_4 in all the remaining lake samples collected from 2012 to 2014 ranged from 4.2 to 618.3 nmol L^{-1} , with a mean of 64.9 ± 92.3 nmol L^{-1} (Figure 3). In the nonmacrophyte-dominated lake regions, dissolved CH_4 decreased notably from the northwestern bays or the western coastal regions to the southeastern lake regions in all hydrological seasons from 2012 to 2014 (Figure 3). Dissolved CH_4 in the river samples ranged from 7.9 to 1597 nmol L^{-1} , with a mean of 307.8 ± 347.5 nmol L^{-1} (Figure 3), and was significantly higher than in the lake samples from the Huxi, Wuchengxiyu, Zhexi, and Hangjiahu subwatersheds in all seasons (t -test, $p < 0.05$; Figure 3; Table S4).

As the temporal resolution of the sampling campaign was seasonal, we found highly depleted $\delta^2\text{H}$ and $\delta^{18}\text{O}$, and enhanced input of terrestrial C2, and thereby high concentrations of dissolved CH_4 , in the northwestern lake regions in November compared with August due to drought on hot August days in the Lake Taihu watershed (Figure 3). An increase in the temporal resolution of the sampling campaign can probably capture the rainy season enhancement of dissolved CH_4 , while in the present results the seasonal enrichment signal was surpassed by the spatial signal.

Significantly higher Chl-*a* concentrations were observed in August (37.8 ± 27.6 $\mu\text{g L}^{-1}$) and November (21.0 ± 18.1 μg

L^{-1}) than in February (9.4 ± 3.8 $\mu\text{g L}^{-1}$; t -test, $p < 0.005$) and May (12.4 ± 7.1 $\mu\text{g L}^{-1}$; t -test, $p < 0.05$). Chl-*a* decreased from the northern regions of the lake to the southeastern bays in all seasons except in February from 2012 to 2014 (Figure 3), coinciding with higher external loading from the northwestern subwatersheds, for instance Huxi and Wuchengxiyu. Chl-*a* in the river samples ranged from 0.5 to 770 $\mu\text{g L}^{-1}$, with a mean of 42.9 ± 74.3 $\mu\text{g L}^{-1}$, and showed no significant difference from the mean Chl-*a* in the lake samples.

Relationships between Dissolved CH_4 and Stable Isotopic, CDOM-Related Indices, Chl-*a*, and Hydrological Indices. Significant positive relationships were found between mean dissolved CH_4 and mean $a(350)$ ($r^2 = 0.11$, $p < 0.001$), DOC ($r^2 = 0.36$, $p < 0.001$), F_{\max} of PARAFAC-derived C1–C3 ($r^2 = 0.07$ – 0.50 , $p < 0.01$), COD ($r^2 = 0.43$, $p < 0.001$), and monthly net inflow runoff (Q_{net}) ($p < 0.001$) (Table S5) for all the samples collected in the lake watershed. It should be noted that the coefficients of determination between mean dissolved CH_4 and mean terrestrial PARAFAC-derived C2 and the products of C2 and Q_{net} , i.e., $Q_{\text{net}} \times \text{C2}$, can be as strong as 0.50 and 0.27, respectively (Table S5). In comparison, significant negative relationships were found between dissolved CH_4 and $a(250)/a(365)$ ($r^2 = 0.14$, $p < 0.001$), $S_{275-295}$ ($r^2 = 0.31$, $p < 0.001$), S_R ($r^2 = 0.28$, $p < 0.001$), stable isotopic $\delta^2\text{H}$ ($r^2 = 0.25$, $p < 0.001$) and $\delta^{18}\text{O}$ ($r^2 = 0.10$, $p < 0.001$), and DO ($r^2 = 0.11$, $p < 0.001$) for all the samples collected (Table S5; Figure S9). No significant relationship emerged between dissolved CH_4 and Chl-*a* or with C4–C6 if all data were used during linear fitting, but exclusion of river samples resulted in significant positive relationships between dissolved CH_4 and Chl-*a* ($r^2 = 0.18$, $p < 0.001$; Figure S9), C4 ($r^2 = 0.10$, $p < 0.001$), and C6 ($r^2 = 0.08$, $p < 0.01$). A close relationship was found between dissolved CH_4 and Chl-*a* if we include only August samples ($r^2 = 0.47$, $p < 0.001$; Figure S10).

Significant positive relationships appeared between mean DOC and mean $a(350)$ ($r^2 = 0.55$, $p < 0.001$), PARAFAC-derived C2–C4 ($r^2 = 0.10$ – 0.62 , $p < 0.001$), COD ($r^2 = 0.69$, $p < 0.001$), net inflow runoff (Q_{net}) ($r^2 = 0.43$, $p < 0.001$), and the product of C2 and Q_{net} , i.e., $Q_{\text{net}} \times \text{C2}$ ($r^2 = 0.56$, $p < 0.001$), in all the samples collected in the lake and the connecting channels (Table S5). Additionally, the coefficient of determination of linear fitting between mean terrestrial C2 and mean DOC can be as high as 0.62 (Table S5). No significant relationship was found between DOC and Chl-*a*, C1, C5, and C6 (Table S5). In comparison, significant negative relationships were observed between mean DOC and mean $a(250)/a(365)$ ($r^2 = 0.30$, $p < 0.001$), $S_{275-295}$ ($r^2 = 0.28$, $p < 0.001$), S_R ($r^2 = 0.26$, $p < 0.001$), stable isotopic $\delta^2\text{H}$ ($r^2 = 0.30$, $p < 0.001$) and $\delta^{18}\text{O}$ ($r^2 = 0.20$, $p < 0.05$), and DO ($r^2 = 0.15$, $p < 0.001$) in all the samples collected (Table S5). When excluding river samples, we further discovered significant positive relationships between terrestrial humic-like C2 and COD ($r^2 = 0.42$, $p < 0.001$) and between C2 and Chl-*a* ($r^2 = 0.18$, $p < 0.001$) and a negative relationship between C2 and DO ($r^2 = 0.15$, $p < 0.001$) (Figure S9).

FT-ICR MS Results. Lignin molecules exhibited 3331, 1802, and 3245 assigned formulas, corresponding to 77, 50, and 68% of the total assigned formulas for the samples collected from the headwater of the Lake Taihu watershed, algal-derived samples, and the central lake, respectively, in November 2016 (Figure 4; Table S6). In comparison, protein-like assigned formulas displayed 214, 897, and 691 peaks,

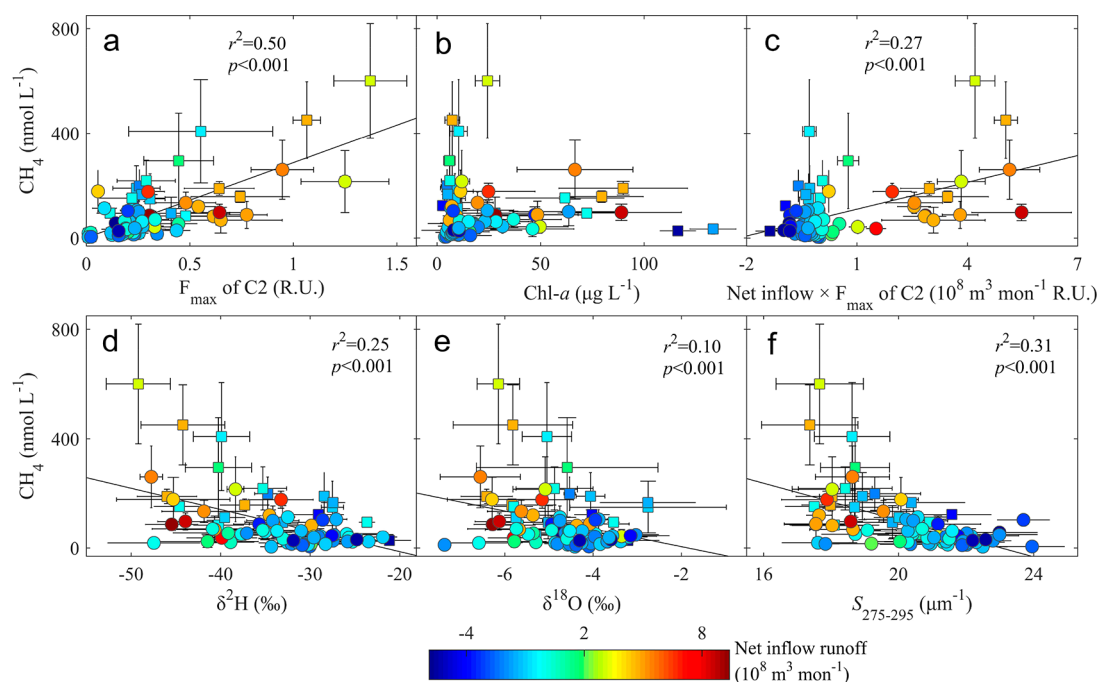


Figure 5. Relationships between mean dissolved CH_4 concentrations and mean F_{max} of terrestrial humic-like C2 (a), Chl- a (b), products of net inflow discharge and F_{max} of C2 (c), $\delta^2\text{H}$ (d), $\delta^{18}\text{O}$ (e), and CDOM absorption spectral slope $S_{275-295}$ (f) in the five subwatersheds. Circles represent samples collected from the lake, while quadrates denote samples collected from the connecting channels. The colored dots display the net inflow discharge in the individual subwatersheds. Error bars in all panels show ± 1 SD of samples collected from different lake regions delineated using white dashed lines as in Figure 1.

corresponding to 5, 25, and 16%, for the headwater, algal-derived, and central lake samples, respectively (Figure 4; Table S6). It is apparent that terrestrial humic-rich lignin molecular formulas have a higher relative abundance than other compound classes assigned to the headwater and the central lake samples (Figure 4; Table S6). In comparison, biological protein-rich molecular formulas have a greater relative abundance than formulas assigned to other compounds for the algal-derived samples (Figure 4; Table S6).

DISCUSSION

Our results indicated that the terrestrial CDOM input likely overrode algal blooms in enhancing dissolved CH_4 levels in large, eutrophic Lake Taihu. First, we found dissolved CH_4 to be highest in the northwestern regions, especially the inflowing river mouths, coinciding with high levels of DOC, terrestrial humic-rich C2–C4, in situ measured terrestrial humic-like fluorophores, and Chl- a (May, August, and November) compared with the southeastern region of the lake (Figures 3 and 4; Figure S7). The significantly higher mean concentrations of dissolved CH_4 in the river samples than in lake samples in the western and northern subwatersheds (Huxi, Wuchengxiyu, Zhexi, and Hangjiahu) in all seasons (Figure 3; Table S4) likely provide further evidence of this. Although upwelling groundwater may enhance the advection of CH_4 to the inflowing channels,⁴⁹ it contributes only a little to the water budget in the lake watershed.²² The discrepancy between the spatial distribution of high values of riverine and lacustrine dissolved CH_4 , especially in the southwestern river mouths (Figure 3), suggested that the dynamics of dissolved CH_4 in the lake itself might not simply reflect the river flow. Moreover, the highly depleted $\delta^2\text{H}$ and $\delta^{18}\text{O}$ and the low $a(250)/a(365)$, $S_{275-295}$, and S_R in the northwestern river mouths (Figure 3;

Figure S7) supported the occurrence of a higher terrestrial contribution here. This is substantiated by $a(250)/a(365)$, $S_{275-295}$, and S_R , which were all negatively related to DOM aromaticity.²⁹ Inflow water discharge usually has depleted $\delta^2\text{H}$ and $\delta^{18}\text{O}$, while enhanced evaporation resulting from a prolonged water retention time in the lake will enrich these isotopes.^{50,51} Second, we found significantly positive relationships between dissolved CH_4 versus $a(350)$, DOC, COD, F_{max} of C1–C3, DOM aromaticity, and net inflow runoff (Q_{net}), as well as $Q_{\text{net}} \times \text{C2}$ for all the samples collected (Figure 5; Table S5). F_{max} of C2 merely denotes the fluorescence intensity of terrestrial humic-like fluorophores, while $Q_{\text{net}} \times \text{C2}$ serves as a surrogate of the loading of terrestrial humic-rich substances. Furthermore, the dissolved CH_4 was negatively related to DO and $\delta^2\text{H}$ and $\delta^{18}\text{O}$ (Figure 5; Table S5).

Microbial and photochemical degradation of the terrestrial humic-like C2 and agricultural humic-like C3 in the northwestern inflowing river mouths and shorelines of the lake likely enhanced the DO depletion observed in these lake regions (Figures 3 and 4; Figure S6), while the relatively high SDD and the low TSM and K_d of underwater light in the UV and PAR ($K_d(\text{PAR})$) regions in the DO-depleted river mouths probably increased the photochemical degradation of CDOM (Figure 4; Figures S6, S8, and S9) and, therefore, potentially also increased the dissolved CH_4 concentrations. This is directly supported by the significant positive relationship between terrestrial CDOM and $K_d(\text{PAR})$ and between K_d of underwater light in the UV and PAR ($K_d(\text{PAR})$) regions (Figure 4; Figure S8). Recent studies demonstrated notably higher SDD and $K_d(\text{PAR})$ in the northwestern than in the remaining lake regions apart from those dominated by macrophytes.^{52,53} Higher UV and PAR light availability in the DO-depleted water column (Figure 4; Figure S8) can lead to mineralization of CDOM to dissolved CH_4 , bioavailable

organic substances, and refractory CDOM^{11,12} in the northwestern inflowing river mouths of the lake. This agrees with the higher SDD and low K_d (PAR) and TSM reported from this area.³⁶ Recent studies have further revealed elevated terrestrial CDOM and nutrient accumulation and enhanced DO depletion in the northwestern part of the lake,^{26,54} which may result in enhanced dissolved CH₄ levels.

Although there were positive relationships between Chl-*a* and dissolved CH₄ when excluding river samples or only examining August samples (Figures S9 and S10), these were weak compared with the relationship between terrestrial C2 and dissolved CH₄ (Figure 5), and the spatial distribution patterns of Chl-*a* and dissolved CH₄ differed in all seasons (Figure 3). This was particularly evident in August and November when there were algal blooms in the northwestern part of the lake but not in the river mouths where high dissolved CH₄ values were recorded (Figure 3). Moreover, the variation in dissolved CH₄ was only weakly related to tryptophan-like C1 (Table S5), which is assumed to be biologically produced from microbial degradation of algal cells.^{26,55,56} From the whole-lake and seasonal perspective, algal degradation was likely not the primary source of dissolved CH₄; however, it might be a significant component of the CH₄ flux in less riverine eutrophic lakes²¹ in summer (Figure S10) or in reservoirs with long water retention time,^{57,58} and in experimental mesocosms.^{59,60} The sporadic aggregation and degradation of massive algal mats in highly eutrophic lake regions may result in black water blooms.^{26,54} This is a phenomenon caused by microbial respiration during the decay of algal mats, resulting in oxygen depletion and with it an expansive area of dark and discolored water with extremely low DO.⁵⁴ Such episodic events are difficult to capture⁵⁴ and would have been expected to lead to CH₄ emission, but this was not considered in the present study because it would most likely have occurred as ebullitive or microbubbling fluxes.^{3,61}

We used dissolved CH₄ concentrations as a surrogate for potential CH₄ emission from Lake Taihu and the connecting channels due to absence of CH₄ emission from the channels. The gas transfer coefficient (k) determined by wind speed and temperature in different lake regions is remarkably uniform, and the emission from the lake is largely controlled by the levels of dissolved CH₄ across the lake²¹ (Figure S1). Our results revealed that six individual fractions differing in spectral shapes characterize the fluorescent properties of CDOM in Lake Taihu and the 51 major channels connecting to it (Figure 2). Dividing CDOM into the six fluorescence components allowed us, in part, to elucidate the potential carbon sources of dissolved CH₄, and it appeared that humic-rich fluorophores derived from terrestrial environments correlated with the levels of dissolved CH₄. Despite the fact that the protein-like fluorescence components C1, C5, and C6 contributed primarily to the fluorescence characteristics of CDOM, dissolved CH₄ was weakly or not correlated with these three components, and DOC was not correlated with them at all (Table S5). In comparison, the humic-like components, C2–C4, likely deriving from the terrestrial environment (e.g., soil organic matter), explained a large proportion of the variability of dissolved CH₄ and predominantly the variability of DOC (Figure 5; Table S5). Headwater and central lake water samples share higher relative abundances of terrestrial lignin molecular formulas identified via FT-ICR MS compared with the algal degradation DOM samples, further suggesting that

DOM in Lake Taihu is primarily of allochthonous origin (Figure 4).

The correlation between terrestrial humic-like substances and dissolved CH₄ in Lake Taihu and the connecting channels does not necessarily prove causation as no information was available on DOM composition of pore water in the sediment where a large fraction of the CH₄ is likely produced.^{5,7} Although the relationship between Chl-*a* and dissolved CH₄ was weak compared with the relationship between terrestrial C2 and dissolved CH₄ during 2012–2014 (Figure 5), the massive algal mats recorded in the northwestern bay during the past three decades²⁴ may enrich the sediment with particulate carbon. The subsequent degradation of particulate organic carbon in the sediment may provide a labile DOM source for methanogens. DOM optical measurements coupled with FT-ICR MS and $\delta^{13}\text{C}$ -DOC can be used to quantify the relative importance of autochthonous and allochthonous DOM^{15,34,62} for CH₄ production at ecosystem scale. Acetoclastic methanogenic archaea have been found at the molecular level in diverse oxygenated aquatic environments where they release CH₄ aerobically.^{63,64} Follow-up experimental work is, therefore, needed to quantify the contribution of DOM degradation to the emission of CH₄ under anaerobic and aerobic conditions.

■ ASSOCIATED CONTENT

📄 Supporting Information

The Supporting Information is available free of charge on the ACS Publications website at DOI: 10.1021/acs.est.8b02163.

Additional information on methods; data including monthly mean inflow and backflow runoff, physico-chemical indices, excitation and emission spectra, temporal variations of daily mean rainfall and monthly inflow and outflow runoff (PDF)

■ AUTHOR INFORMATION

Corresponding Author

*Phone: +86-25-86882198, fax: +86-25-57714759. email: ylzhang@niglas.ac.cn.

ORCID

Yongqiang Zhou: 0000-0003-1402-345X

David C. Podgorski: 0000-0002-1070-5923

Author Contributions

Yongqiang Zhou and Qitao Xiao: These authors contributed equally to the manuscript.

Notes

The authors declare no competing financial interest.

■ ACKNOWLEDGMENTS

This study was jointly funded by the National Natural Science Foundation of China (Grants 41621002, 41807362, and 41661134036), the Provincial Natural Science Foundation of Jiangsu in China (BK20181104), NIGLAS Cross-functional Innovation Teams (NIGLAS2016TD01), and NIGLAS Foundation (NIGLAS2017QD08). Erik Jeppesen was supported by the MARS project (Managing Aquatic ecosystems and water Resources under multiple Stress) funded under the seventh EU Framework Programme, Theme 6 (Environment including Climate Change), Contract No. 603378 (<http://www.mars-project.eu>), and the AU Centre for Water Technology (WATEC). FT-ICR MS measurement was supported by the National Science Foundation (DMR-

1157490). We would like to express our deep thanks to Anne Mette Poulsen from Aarhus University for editorial assistance. We would also like to thank Zhiqiang Shi, Mingzhu Wang, Wei Xiao, Wei Wang, Xiaohan Liu, Jingchen Xue, Zhong Xia, Phoebe Zito, and Chengyang Zhang for their help with field sample collection and laboratory measurements. We thank the editor Dr. Xiangdong Li and the four anonymous reviewers for their very constructive comments.

REFERENCES

- (1) Davidson, T. A.; Audet, J.; Svenning, J. C.; Lauridsen, T. L.; Sondergaard, M.; Landkildehus, F.; Larsen, S. E.; Jeppesen, E. Eutrophication effects on greenhouse gas fluxes from shallow-lake mesocosms override those of climate warming. *Global Change Biology* **2015**, *21* (12), 4449–4463.
- (2) Wit, F.; Muller, D.; Baum, A.; Warneke, T.; Pranowo, W. S.; Muller, M.; Rixen, T. The impact of disturbed peatlands on river outgassing in Southeast Asia. *Nat. Commun.* **2015**, *6*, 10155.
- (3) Davidson, T. A.; Audet, J.; Jeppesen, E.; Landkildehus, F.; Lauridsen, T. L.; Sondergaard, M.; Syväranta, J. Synergy between nutrients and warming enhances methane ebullition from experimental lakes. *Nat. Clim. Change* **2018**, *8*, 156–160.
- (4) Samad, M. S.; Bertilsson, S. Seasonal variation in abundance and diversity of bacterial methanotrophs in five temperate lakes. *Front. Microbiol.* **2017**, *8*, 142.
- (5) Wik, M.; Varner, R. K.; Anthony, K. W.; MacIntyre, S.; Bastviken, D. Climate-sensitive northern lakes and ponds are critical components of methane release. *Nat. Geosci.* **2016**, *9* (2), 99–105.
- (6) Michaud, A. B.; Dore, J. E.; Achberger, A. M.; Christner, B. C.; Mitchell, A. C.; Skidmore, M. L.; Vick-Majors, T. J.; Priscu, J. C. Microbial oxidation as a methane sink beneath the West Antarctic Ice Sheet. *Nat. Geosci.* **2017**, *10* (8), 582–586.
- (7) Thauer, R. K.; Kaster, A.-K.; Seedorf, H.; Hedderich, R.; Buckel, W. Methanogenic archaea: ecologically relevant differences in energy conservation. *Nat. Rev. Microbiol.* **2008**, *6* (8), 579–591.
- (8) Bogard, M. J.; del Giorgio, P. A.; Boutet, L.; Chaves, M. C. G.; Prairie, Y. T.; Merante, A.; Derry, A. M. Oxidic water column methanogenesis as a major component of aquatic CH₄ fluxes. *Nat. Commun.* **2014**, *5*, 5350.
- (9) Repeta, D. J.; Ferrón, S.; Sosa, O. A.; Johnson, C. G.; Repeta, L. D.; Acker, M.; DeLong, E. F.; Karl, D. M. Marine methane paradox explained by bacterial degradation of dissolved organic matter. *Nat. Geosci.* **2016**, *9* (12), 884–887.
- (10) Cory, R. M.; Crump, B. C.; Dobkowski, J. A.; Kling, G. W. Surface exposure to sunlight stimulates CO₂ release from permafrost soil carbon in the Arctic. *Proc. Natl. Acad. Sci. U. S. A.* **2013**, *110* (9), 3429–3434.
- (11) Cory, R. M.; Ward, C. P.; Crump, B. C.; Kling, G. W. Sunlight controls water column processing of carbon in arctic fresh waters. *Science* **2014**, *345* (6199), 925–928.
- (12) Bange, H. W.; Uher, G. Photochemical production of methane in natural waters: implications for its present and past oceanic source. *Chemosphere* **2005**, *58* (2), 177–83.
- (13) Kothawala, D. N.; Stedmon, C. A.; Muller, R. A.; Weyhenmeyer, G. A.; Kohler, S. J.; Tranvik, L. J. Controls of dissolved organic matter quality: evidence from a large-scale boreal lake survey. *Global Change Biology* **2014**, *20* (4), 1101–1114.
- (14) Kellerman, A. M.; Dittmar, T.; Kothawala, D. N.; Tranvik, L. J. Chemodiversity of dissolved organic matter in lakes driven by climate and hydrology. *Nat. Commun.* **2014**, *5*, 3804.
- (15) Kellerman, A. M.; Kothawala, D. N.; Dittmar, T.; Tranvik, L. J. Persistence of dissolved organic matter in lakes related to its molecular characteristics. *Nat. Geosci.* **2015**, *8* (6), 454–457.
- (16) Zhou, Y.; Zhang, Y.; Jeppesen, E.; Murphy, K. R.; Shi, K.; Liu, M.; Liu, X.; Zhu, G. Inflow rate-driven changes in the composition and dynamics of chromophoric dissolved organic matter in a large drinking water lake. *Water Res.* **2016**, *100*, 211–221.
- (17) Zhang, Y.; Yin, Y.; Feng, L.; Zhu, G.; Shi, Z.; Liu, X.; Zhang, Y. Characterizing chromophoric dissolved organic matter in Lake Tianmuhu and its catchment basin using excitation-emission matrix fluorescence and parallel factor analysis. *Water Res.* **2011**, *45* (16), 5110–5122.
- (18) Bianchi, T. S. The role of terrestrially derived organic carbon in the coastal ocean: A changing paradigm and the priming effect. *Proc. Natl. Acad. Sci. U. S. A.* **2011**, *108* (49), 19473–19481.
- (19) Stedmon, C. A.; Thomas, D. N.; Granskog, M.; Kaartokallio, H.; Papadimitriou, S.; Kuosa, H. Characteristics of dissolved organic matter in Baltic coastal sea ice: allochthonous or autochthonous origins? *Environ. Sci. Technol.* **2007**, *41* (21), 7273–7279.
- (20) Conrad, R. The global methane cycle: recent advances in understanding the microbial processes involved. *Environ. Microbiol. Rep.* **2009**, *1* (5), 285–92.
- (21) Xiao, Q.; Zhang, M.; Hu, Z.; Gao, Y.; Hu, C.; Liu, C.; Liu, S.; Zhang, Z.; Zhao, J.; Xiao, W.; Lee, X. Spatial variations of methane emission in a large shallow eutrophic lake in subtropical climate. *J. Geophys. Res.: Biogeosci.* **2017**, *122* (7), 1597–1614.
- (22) Zhou, Y.; Yao, X.; Zhang, Y.; Zhang, Y.; Shi, K.; Tang, X.; Qin, B.; Podgorski, D. C.; Brookes, J. D.; Jeppesen, E. Response of dissolved organic matter optical properties to net inflow runoff in a large fluvial plain lake and the connecting channels. *Sci. Total Environ.* **2018**, *639*, 876–887.
- (23) Tang, X.; Gao, G.; Chao, J.; Wang, X.; Zhu, G.; Qin, B. Dynamics of organic-aggregate-bacterial communities and related environmental factors in Lake Taihu, a large eutrophic shallow lake in China. *Limnol. Oceanogr.* **2010**, *55* (2), 469–480.
- (24) Qin, B.; Xu, P.; Wu, Q.; Luo, L.; Zhang, Y. Environmental issues of Lake Taihu, China. *Hydrobiologia* **2007**, *581* (1), 3–14.
- (25) Niu, C.; Zhang, Y.; Zhou, Y.; Shi, K.; Liu, X.; Qin, B. The potential applications of real-time monitoring of water quality in a large shallow lake (Lake Taihu, China) using a chromophoric dissolved organic matter fluorescence sensor. *Sensors* **2014**, *14* (7), 11580–11594.
- (26) Zhou, Y.; Jeppesen, E.; Zhang, Y.; Niu, C.; Shi, K.; Liu, X.; Zhu, G.; Qin, B. Chromophoric dissolved organic matter of black waters in a highly eutrophic Chinese lake: Freshly produced from algal scums? *J. Hazard. Mater.* **2015**, *299*, 222–230.
- (27) Xiao, W.; Wen, X.; Wang, W.; Xiao, Q.; Xu, J.; Cao, C.; Xu, J.; Hu, C.; Shen, J.; Liu, S.; Lee, X. Spatial distribution and temporal variability of stable water isotopes in a large and shallow lake. *Isot. Environ. Health Stud.* **2016**, *52* (4–5), 443–454.
- (28) Spencer, R. G. M.; Aiken, G. R.; Dornblaser, M. M.; Butler, K. D.; Holmes, R. M.; Fiske, G.; Mann, P. J.; Stubbins, A. Chromophoric dissolved organic matter export from U.S. rivers. *Geophys. Res. Lett.* **2013**, *40* (8), 1575–1579.
- (29) Helms, J. R.; Stubbins, A.; Ritchie, J. D.; Minor, E. C.; Kieber, D. J.; Mopper, K. Absorption spectral slopes and slope ratios as indicators of molecular weight, source, and photobleaching of chromophoric dissolved organic matter. *Limnol. Oceanogr.* **2008**, *53* (3), 955–969.
- (30) Fichot, C. G.; Benner, R. The spectral slope coefficient of chromophoric dissolved organic matter (S_{275–295}) as a tracer of terrigenous dissolved organic carbon in river-influenced ocean margins. *Limnol. Oceanogr.* **2012**, *57* (5), 1453–1466.
- (31) Stedmon, C. A.; Markager, S.; Bro, R. Tracing dissolved organic matter in aquatic environments using a new approach to fluorescence spectroscopy. *Mar. Chem.* **2003**, *82* (3–4), 239–254.
- (32) Murphy, K. R.; Stedmon, C. A.; Waite, T. D.; Ruiz, G. M. Distinguishing between terrestrial and autochthonous organic matter sources in marine environments using fluorescence spectroscopy. *Mar. Chem.* **2008**, *108* (1–2), 40–58.
- (33) Dittmar, T.; Koch, B.; Hertkorn, N.; Kattner, G. A simple and efficient method for the solid-phase extraction of dissolved organic matter (SPE-DOM) from seawater. *Limnol. Oceanogr.: Methods* **2008**, *6*, 230–235.
- (34) Spencer, R. G. M.; Guo, W.; Raymond, P. A.; Dittmar, T.; Hood, E.; Fellman, J.; Stubbins, A. Source and biolability of ancient

dissolved organic matter in glacier and lake ecosystems on the Tibetan Plateau. *Geochim. Cosmochim. Acta* **2014**, *142*, 64–74.

(35) Kellerman, A. M.; Guillemette, F.; Podgorski, D. C.; Aiken, G. R.; Butler, K. D.; Spencer, R. G. M. Unifying concepts linking dissolved organic matter composition to persistence in aquatic ecosystems. *Environ. Sci. Technol.* **2018**, *52* (5), 2538–2548.

(36) Ohno, T.; Parr, T. B.; Gruselle, M. C.; Fernandez, I. J.; Sleighter, R. L.; Hatcher, P. G. Molecular composition and biodegradability of soil organic matter: a case study comparing two new England forest types. *Environ. Sci. Technol.* **2014**, *48* (13), 7229–7236.

(37) Murphy, K. R.; Stedmon, C. A.; Wenig, P.; Bro, R. OpenFluor—an online spectral library of auto-fluorescence by organic compounds in the environment. *Anal. Methods* **2014**, *6* (3), 658–661.

(38) Murphy, K. R.; Hambly, A.; Singh, S.; Henderson, R. K.; Baker, A.; Stuetz, R.; Khan, S. J. Organic matter fluorescence in municipal water recycling schemes: Toward a unified PARAFAC model. *Environ. Sci. Technol.* **2011**, *45* (7), 2909–2916.

(39) Stedmon, C. A.; Markager, S. Resolving the variability in dissolved organic matter fluorescence in a temperate estuary and its catchment using PARAFAC analysis. *Limnol. Oceanogr.* **2005**, *50* (2), 686–697.

(40) Shutova, Y.; Baker, A.; Bridgeman, J.; Henderson, R. K. Spectroscopic characterisation of dissolved organic matter changes in drinking water treatment: From PARAFAC analysis to online monitoring wavelengths. *Water Res.* **2014**, *54*, 159–169.

(41) Williams, C. J.; Yamashita, Y.; Wilson, H. F.; Jaffé, R.; Xenopoulos, M. A. Unraveling the role of land use and microbial activity in shaping dissolved organic matter characteristics in stream ecosystems. *Limnol. Oceanogr.* **2010**, *55* (3), 1159–1171.

(42) Kowalczyk, P.; Durako, M. J.; Young, H.; Kahn, A. E.; Cooper, W. J.; Gonsior, M. Characterization of dissolved organic matter fluorescence in the South Atlantic Bight with use of PARAFAC model: Interannual variability. *Mar. Chem.* **2009**, *113* (3–4), 182–196.

(43) Osburn, C. L.; Handsel, L. T.; Mikan, M. P.; Paerl, H. W.; Montgomery, M. T. Fluorescence tracking of dissolved and particulate organic matter quality in a river-dominated estuary. *Environ. Sci. Technol.* **2012**, *46* (16), 8628–8636.

(44) Osburn, C. L.; Wigdahl, C. R.; Fritz, S. C.; Saros, J. E. Dissolved organic matter composition and photoreactivity in prairie lakes of the U.S. Great Plains. *Limnol. Oceanogr.* **2011**, *56* (6), 2371–2390.

(45) Jørgensen, L.; Stedmon, C. A.; Kragh, T.; Markager, S.; Middelboe, M.; Sondergaard, M. Global trends in the fluorescence characteristics and distribution of marine dissolved organic matter. *Mar. Chem.* **2011**, *126* (1–4), 139–148.

(46) Kowalczyk, P.; Tilstone, G. H.; Zablocka, M.; Röttgers, R.; Thomas, R. Composition of dissolved organic matter along an Atlantic Meridional Transect from fluorescence spectroscopy and parallel factor analysis. *Mar. Chem.* **2013**, *157*, 170–184.

(47) Dong, B.; Qin, B.; Gao, G.; Cai, X. Submerged macrophyte communities and the controlling factors in large, shallow Lake Taihu (China): Sediment distribution and water depth. *J. Great Lakes Res.* **2014**, *40* (3), 646–655.

(48) Liu, X.; Zhang, Y.; Shi, K.; Zhou, Y.; Tang, X.; Zhu, G.; Qin, B. Mapping aquatic vegetation in a large, shallow eutrophic lake: A frequency-based approach using multiple years of MODIS data. *Remote Sensing* **2015**, *7* (8), 10295–10320.

(49) Sherwood, O. A.; Rogers, J. D.; Lackey, G.; Burke, T. L.; Osborn, S. G.; Ryan, J. N. Groundwater methane in relation to oil and gas development and shallow coal seams in the Denver-Julesburg Basin of Colorado. *Proc. Natl. Acad. Sci. U. S. A.* **2016**, *113* (30), 8391–8396.

(50) Wu, H.; Li, X.; Li, J.; Jiang, Z.; Li, G.; Liu, L. Evaporative enrichment of stable isotopes ($\delta^{18}\text{O}$ and δD) in lake water and the relation to lake-level change of Lake Qinghai, Northeast Tibetan Plateau of China. *Journal of Arid Land* **2015**, *7* (5), 623–635.

(51) Yamamoto-Kawai, M.; McLaughlin, F. A.; Carmack, E. C.; Nishino, S.; Shimada, K. Freshwater budget of the Canada Basin,

Arctic Ocean, from salinity, $\delta^{18}\text{O}$, and nutrients. *J. Geophys. Res.* **2008**, *113*, C01007.

(52) Liu, X.; Zhang, Y.; Shi, K.; Lin, J.; Zhou, Y.; Qin, B. Determining critical light and hydrologic conditions for macrophyte presence in a large shallow lake: The ratio of euphotic depth to water depth. *Ecol. Indic.* **2016**, *71*, 317–326.

(53) Shi, K.; Zhang, Y.; Liu, X.; Wang, M.; Qin, B. Remote sensing of diffuse attenuation coefficient of photosynthetically active radiation in Lake Taihu using MERIS data. *Remote Sensing of Environment* **2014**, *140*, 365–377.

(54) Zhang, Y.; Shi, K.; Liu, J.; Deng, J.; Qin, B.; Zhu, G.; Zhou, Y. Meteorological and hydrological conditions driving the formation and disappearance of black blooms, an ecological disaster phenomena of eutrophication and algal blooms. *Sci. Total Environ.* **2016**, *569–570*, 1517–1529.

(55) Stedmon, C. A.; Markager, S. Tracing the production and degradation of autochthonous fractions of dissolved organic matter by fluorescence analysis. *Limnol. Oceanogr.* **2005**, *50* (5), 1415–1426.

(56) Zhang, Y.; van Dijk, M. A.; Liu, M.; Zhu, G.; Qin, B. The contribution of phytoplankton degradation to chromophoric dissolved organic matter (CDOM) in eutrophic shallow lakes: Field and experimental evidence. *Water Res.* **2009**, *43* (18), 4685–4697.

(57) Deemer, B. R.; Harrison, J. A.; Li, S.; Beaulieu, J. J.; Delsontro, T.; Barros, N.; Bezerraneto, J. F.; Powers, S. M.; dos Santos, M. A.; Vonk, J. A. Greenhouse Gas Emissions from Reservoir Water Surfaces: A New Global Synthesis. *BioScience* **2016**, *66* (11), 949–964.

(58) Beaulieu, J. J.; Mcmanus, M. G.; Nietch, C. T. Estimates of reservoir methane emissions based on a spatially balanced probabilistic-survey. *Limnol. Oceanogr.* **2016**, *61*, S27–S40.

(59) West, W. E.; Coloso, J. J.; Jones, S. E. Effects of algal and terrestrial carbon on methane production rates and methanogen community structure in a temperate lake sediment. *Freshwater Biol.* **2012**, *57* (5), 949–955.

(60) West, W. E.; Mccarthy, S. M.; Jones, S. E. Phytoplankton lipid content influences freshwater lake methanogenesis. *Freshwater Biol.* **2015**, *60* (11), 2261–2269.

(61) Feng, Z.; Fan, C.; Huang, W.; Ding, S. Microorganisms and typical organic matter responsible for lacustrine “black bloom”. *Sci. Total Environ.* **2014**, *470–471*, 1–8.

(62) Drake, T. W.; Raymond, P. A.; Spencer, R. G. M. Terrestrial carbon inputs to inland waters: A current synthesis of estimates and uncertainty. *Limnology and Oceanography Letters* **2018**, *3*, 132–142.

(63) Grossart, H. P.; Frindte, K.; Dziallas, C.; Eckert, W.; Tang, K. W. Microbial methane production in oxygenated water column of an oligotrophic lake. *Proc. Natl. Acad. Sci. U. S. A.* **2011**, *108* (49), 19657–19661.

(64) Carini, P.; White, A. E.; Campbell, E. O.; Giovannoni, S. J. Methane production by phosphate-starved SAR11 chemoheterotrophic marine bacteria. *Nat. Commun.* **2014**, *5*, 4346.